Periodontal tissue regeneration by transplantation of adipose-derived stromal cells in combination with PLGA-based solid scaffolds

Nihon University Graduate School of Dentistry

Daisuke Akita

(Directors : Profs. Tomohiko Ishigami and Keitaro Isokawa, and

Assoc. Profs. Masaki Honda and Naoki Tsukimura)

Contents

Basic Article

Akita D, Morokuma M, Saito Y, Yamanaka K, Akiyama Y, Sato M, Mashimo T, Toriumi T, Arai Y, Kaneko T, Tsukimura N, Isokawa K, Ishigami T and Honda MJ (2014) Periodontal tissue regeneration by transplantation of rat adipose-derived stromal cells in combination with PLGA-based solid scaffolds. Biomed Res. Vol. 35, No. 2 (in press).

Abstract

Regeneration of damaged periodontium is challenging due to its multi-tissue composition. Mesenchymal stem cell-based approaches using adipose-derived stromal cells (ASCs) may contribute to periodontal reconstruction, particularly when combined with the use of scaffolds to maintain a space for new tissue growth. The aim of this study was to assess the regenerative potential of ASCs derived from inbred or outbred rats in combination with novel solid scaffolds composed of PLGA (poly *d, l*-lactic-co-glycolic acid) (PLGA-scaffolds). ASCs, which could show adipogenic, chondrogenic and osteogenic differenciation, were seeded onto PLGA-scaffolds (ASCs/PLGA). ASCs/PLGA and PLGA alone were transplanted into periodontal fenestration defects created in F344 or Sprague Dawley (SD) rats. Micro-CT analysis showed a significantly higher percentage of bone growth in the ASCs/PLGA groups compared with the PLGA-alone groups at five weeks after surgery. Similarly, histomorphometric analysis demonstrated thicker growth of periodontal ligament and cementum layers in the ASCs/PLGA-groups compared with the PLGA-alone groups. In addition, transplanted DiI-labeled ASCs were observed in the periodontal regenerative sites. The present investigation demonstrated a significant potential of ASCs/PLGA in repairing periodontal defects.

Introduction

Periodontitis is a common inflammatory disease of the dental region, resulting in loss of periodontium and tooth loss. Various surgical procedures such as guided tissue regeneration or use of enamel matrix derivatives have been applied to facilitate regeneration of lost or diseased periodontal tissues (12, 13, 31, 43, 44). However, it is often difficult to achieve a complete reconstruction of the affected periodontal tissue since this tissue is composed of different cell types and elements (6, 56). A tissue engineering approach to regenerate periodontium may have advantages over conventional regenerative procedures because it involves the recruitment of stem/progenitor cells, with their necessary signaling capabilities, in combination with a prefabricated three-dimensional scaffold (41). An extensive study of periodontal tissue regeneration has identified the essential factors to be appropriate progenitor/stem cells, necessary signaling molecules, an extracellular matrix or scaffold as carrier, and an adequate blood supply (27).

Mesenchymal stem cells (MSCs) present in a number of postnatal tissues appear to be an ideal cell source for tissue engineering because of their simple isolation techniques, easy expandability, and multipotency (45, 47, 49, 51, 66). Although MSCs are available from various tissues, the problems include a low number of harvested cells and limited availability of harvested tissues. Therefore, to satisfy efficacy and safety requirements, almost all adult-derived MSCs require at least some degree of *ex vivo* expansion or further manipulation before they can be used clinically.

In recent years, adipose tissue-derived stromal cells (ASCs) have been widely studied as potential stem cells in regenerative medicine because subcutaneous adipose tissues are easily obtained in large quantities (41). ASCs have similar characteristics to bone marrow-derived MSCs (9-11, 16, 23, 28, 40, 46, 51, 52, 65, 66). In addition, ASCs have several advantages over MSCs, including ease of isolation, relative abundance, and rapid expansion capability (65). Furthermore, since ASCs secrete several cytokines including vascular endothelial growth factor (VEGF), hepatocyte growth factor (HGF), and fibroblast growth factor (FGF), all of which function as angiogenic growth factors, ASCs can differentiate into endothelial cells (22, 48, 63) and thereby enhance the blood supply to transplanted grafts (34). These characteristics suggest that ASCs would be useful as autologous transplant cells for tissue regeneration (11). In fact, several reports of ASCs transplantation for periodontal tissue engineering suggested that these stem cells have the potential to regenerate cementum, alveolar bone, and periodontal ligament structures (53-55).

Three-dimensional (3D) scaffolds are widely recognized as essential for many tissue engineering applications. The most extensively used synthetic polymers in tissue engineering studies are poly (glycolic acid), poly (lactic acid), and their copolymers [e.g., (poly *d, l*-lactic-co-glycolic acid; PLGA)], which typically offer a higher primary stability and are more amenable to macro/micro-structure

formation than natural biomaterials. Previous studies in periodontal tissue engineering demonstrated the value of transplanting ASCs with platelet-rich plasma; however, there is no report of other materials used in combination with ASCs in the study of periodontal tissue regeneration (54, 55). A biodegradable PLGA-polymer sponge has been used to deliver cementoblasts in a rat periodontal fenestration model, with the transplanted cementoblasts showing the potential to generate the mineralization (64). A biodegradable scaffold would seem necessary for the delivery of stem/progenitor cells to the periodontal defect, both to preserve space for the formation of new periodontal tissue and to initially support the growing transplanted cells (57). This study thus sought to evaluate the *in vivo* potential for periodontal tissue regeneration with rat-derived ASCs in combination with a biodegradable scaffold. An additional aim was to assess the potential of allogenic rat-derived ASCs to regenerate periodontal tissues as demonstrated in previous studies (14, 54).

Materials and Methods

1. Experimental animals

All animal experiments were performed according to the guidelines for Animal Research and Care Committee at the Nihon University School of Dentistry. The 9-week-old male F344 rats and 8-week-old male Sprague-Dawley (SD) normal rats were purchased from CLEA Japan, Inc (Tokyo, Japan).

2. Isolation and culture of adipose tissue-derived stromal cells

Adipose tissues obtained from inbred F344 rats (males, 9 weeks) and outbred male SD rats (males, 8 weeks) were processed to isolate the ASC population, as described previously (14, 54, 65). Briefly, approximately 1 g of rat inguinal fat pads was harvested, washed extensively with phosphate-buffered saline (PBS), minced for 10 min with fine scissors, and enzymatically digested with 0.1% (w/v) collagenase solution (C6885; Sigma-Aldrich, St. Louis, MO) at 37°C for 1 h. After neutralizing the collagenase activity, the pellet was treated with PBS for 10 min to lyse red blood cells. The remaining cells were plated in DMEM supplemented with 10% fetal bovine serum (FBS) and 1% antibiotics as a growth medium. The cells were referred to as stromal vascular fraction cells which were cultured at 37°C in a humidified atmosphere containing 5% CO_2. Twenty-four hours after plating, all non-adherent cells were removed by washing and the plastic adherent cells were named ASCs. The medium was changed every 3 days. After reaching 80% confluence, the cells were cultured at a ratio of 1:3 in the growth medium. All cells were used at the second or third culturing passage.

3. Differentiation assays

Adipogenesis was induced as previously described (35, 36). For adipogenic differentiation, cells obtained from F344 and SD rats were plated in 6-well plate dishes at a density of 5×10^4 cells and grown to confluency with growth medium. The cells were then incubated for 3 weeks in DMEM containing 10% FBS, 1 mM dexamethasone (Sigma-Aldrich), 0.5 mM isobutylmethylxanthine (Sigma-Aldrich), and 1× insulin-transferrin-selenium-A (ITS; GIBCO-Life Technologies) as an adipogenic induction medium. Lipid vacuole formation in the cells was determined by Oil red O staining after 21 days in the adipogenic induction medium. The cells were fixed for 10 min with 10% neutral buffered paraformaldehyde, incubated with 60% isopropanol for 1 min, and stained with Oil red O working solution (Wako Pure Chemical Industries) for 15 min. Each test was conducted three times.

For osteogenic differentiation, cells obtained from both F344 and SD rats were plated in 6-well plate dishes at a density of 5×10^4 cells and grown to confluency with growth medium. The growth medium was replaced with osteogenic induction medium including DMEM containing 10% FBS, 100 nM dexamethasone, 10 mM glycerol 2-phosphate disodium salt hydrate (Sigma-Aldrich), and 50 mM L-ascorbic acid phosphate magnesium salt *n*-Hydrate (Wako Pure Chemical Industries). The cells were cultured with the

osteogenic induction medium for 21 days, fixed for 10 min with 10% neutral buffered paraformaldehyde and stained with alkaline phosphatase (ALP) activity using NBT/BCIP ready-to-use tablets, pH 9.5 (Roche Diagnostics, Pentzberg, Germany) for 45 min. In addition, for the detection of calcium deposition, cells were incubated in 1% Alizarin Red S (Sigma-Aldrich) for 3 min. Ca^{2+} accumulation was also determined by measuring Ca^{2+} uptake at 21 days after replacing the osteogenic induction medium. The culture supernatant was removed and cells were washed with PBS, 1 M HCl solution was added to each well and 500 μL of distilled water was added to each well. The amount of Ca^{2+} was determined using the Calcium E-test according to the manufacturer's instructions (Wako Pure Chemical Industries). Each test was conducted three times and results were presented as the mean ± standard deviation.

For chondrogenic differentiation, cell pellets obtained from F344 were collected in centrifuge tube (2.5×10^4 cells/tube) with growth medium. After 2 days in culture, the growth medium was replaced with chondrogenic induction medium including DMEM containing 1% FBS, 50 μM L-ascorbic acid phosphate magnesium salt *n*-Hydrate, 40 μg/mL proline (Sigma-Aldrich), 100 μg/mL pyruvate (Sigma-Aldrich), 10 ng/mL recombinant human TGF-β3 (R&D Systems, Inc., Minneapolis, MN, USA), and 1 × ITS for 21 days. The microscopic structure of cells was examined after cell pellets were fixed for 10 min with 10% neutral buffered paraformaldehyde, dehydrated in a series of ethanol, embedded in paraffin, and cut into 7 μm sections. After deparaffinization of sections they were stained with Alcian Blue (0.1 N, pH 1.0).

4. Preparation of scaffolds

PLGA (LA:GA = 75:25, Mw. 25 kDa) sponges were fabricated using a previously described solvent casting-particulate leaching technique (26). In this process, PLGA particles were dissolved in 1, 4-dioxane (Wako), to yield an 8% (w/v) solution. Following solvent evaporation, polymer films with entrapped salt particles (thickness 3 mm) were carefully removed from the molds. The salt was removed by immersing films in distilled water for 48 h. PLGA sponges were then crushed and sieved to yield a range of sizes. The powder was loaded into a stainless disk mold (diameter 5 mm; FTC, Chiba, Japan) and heat pressed (70°C, 5 min) to yield solid scaffold with a thickness of 2 mm. In this process, porosity was adjusted in the quantity of the powder to load. Before cell seeding, the disks were sterilized by γ-ray irradiation.

The PLGA-based solid scaffolds (PLGA-scaffold), with a porosity of 80~90%, were resized to approximately $2 \times 3 \times 1$ mm^3 soaked in 70% ethanol for 30 min to improve wetting, and then a vacuum pump was used to remove the air bubbles. The scaffolds were then washed three times (30 min each) in PBS to remove the residual ethanol. Finally, the scaffolds were washed twice with growth medium (2 h each).

Morphological analysis of PLGA-scaffold was undertaken using a scanning electron microscope (SEM; TM-3000, Hitachi High-Technologies, Tokyo, Japan) to determine the pore size (Fig. 1). After rinsing three times with 0.1 M sodium cacodylate buffer for 15 min each, scaffolds were dehydrated using a graded series of ethanol solutions (35%, 50%, 70%, 80%, 95%, and 100% for 20 min each). After

the final wash, hexamethyldisazane was added for 10 min. Each PLGA-scaffold was then air dried and mounted on stubs, carbon-coated by sputter deposition, and then examined by SEM.

5. Cell seeding methods

One hundred-μL aliquots of the cell suspension (1×10^7 cells/mL, 1×10^6 cells/scaffold) were seeded onto the tops of prewetted PLGA-scaffolds placed on water absorption filter paper (30 × 30 × 5 mm) (Bio-RAD, LA, USA). The PLGA-scaffolds were left undisturbed in an incubator for 1 h to allow the cells to attach. Approximately 5×10^4 cells were seeded onto each PLGA-scaffold. These were then placed upside down and cultured in an incubator at 37 °C with 5% CO_2 for approximately 1 h. As a negative control, empty PLGA-scaffolds were prepared simultaneously, but without addition of the cell suspension.

6. Periodontal fenestration defect model and transplantation

The rat periodontal fenestration defect model was prepared as previously described (14, 25, 61). Nine-week-old F344 (n = 4) and 8-week-old SD rats (n = 3) were anesthetized by intraperitoneal infusion of sodium pentobarbital (30 mg/kg; Somnopentyl; Schering-Plough, Munich, Germany). A skin incision was made along the inferior border of the mandible, then the masseter muscle and the periosteum covering the buccal surface of the mandible were elevated as a flap. The alveolar bone overlying the mandibular 1st and 2nd molar roots was removed with a dental inverted bur. The size of periodontal defect was approximately 2 × 3 × 1 mm in height, width and depth, respectively, with the anterior margin mesial to the distal root of the 1st molar and the posterior margin just distal of the 2nd molar. The coronal margin was approximately 1.5 mm apical of the crest of the alveolar bone and the inferior margin was approximately 2.5 mm apical of the alveolar crest (Fig. 2A, 2B and 2C). The exposed roots of the first and second molars were denuded of their periodontal ligament and cementum (Fig. 2D). PLGA-scaffolds with ASCs (ASCs/PLGA group) were placed in the defects and covered with GC membrane (GC Dental Product Co. Ltd). After the masseter muscle was repositioned, the skin incision was closed to ensure healing by primary intention. Control sites received the PLGA-scaffolds covered with GC membrane without ASCs (PLGA group).

7. *In vivo* X-ray micro computed tomography (micro-CT) analysis

This study used *in vivo* X-ray micro computed tomography (R_mCT; Rigaku Corporation, Tokyo, Japan). The exposure parameters were 17 s, 90 kV, and 100 μA. The voxel size is the isotropic of 30 μm.

Hard tissue regeneration images were obtained from individual rats immediately after surgery (0 week) and at 1, 2 and 5 weeks after surgery with time. The images were taken and constructed into three-dimensional images using i-View (J. Morita Co., Kyoto, Japan). Bone volume was measured within the regions of interest (ROI) from voxel images using bone volume-measuring software 3by4viewer2011 (Kitasenjyu Radist Dental Clinic I-View Image Center, Tokyo, Japan).

The ROI size was 4 × 3 × 1.5 mm, which covered the surgically created periodontal tissue defect. The bone volume in the ROI was measured on day 0 and again each week. The increase in bone volume in individual rats was then

calculated by subtracting the bone volume on day 0 from each of the subsequent values. The increase in bone was considered to be defect re-ossification. Thus, the calculated values indicate re-ossification bone volume immediately at 0, 1, 2, and 5 weeks after surgery (n = 4 from F344 and n = 3 from SD rats).

8. Histological observation and histometric analysis

Five weeks after surgery, the harvested specimens were fixed in 10% neutral buffered paraformaldehyde for 24 h, decalcified in 10% EDTA for 5 weeks, dehydrated through a graded ethanol series, and then embedded in paraffin. For the F344 rat specimens (n = 4), frontal plane sections (thickness 7 μm) were prepared with a microtome (Leica RM2165, Nussloch, Germany) and the paraffin sections were stained with haematoxylin and eosin (H-E). To observe the periodontal ligament fibers and Sharpey's fibers, the first molar distal root sections were stained with Picro Sirius Red.

For the quantitative analysis, five H-E-stained sections per specimen were selected and the thickness of newly formed cementum and periodontium was evaluated by light microscope (ECLIPSE LV100POL, Nikon, Tokyo, Japan) in the three parts (crown, central, and root apex areas) separated in the created periodontal defects.

For the specimens obtained from SD rats (n = 3), horizontal sections (thickness 7 μm) were prepared with a microtome and the paraffin sections were stained with H-E. In addition, the sections were stained with Picro Sirius red to observe collagen fibers attached to the newly formed cementum-like tissues.

9. Localization of DiI-labeled adipose-derived stromal cells

According to the manufacturer's instructions, harvested cells derived from F344 rats with 0.25% Trypsin-EDTA were resuspended at 1×10^6 cells/ml in DMEM, and labeled with the fluorescent dye, chloromethylbenzamido 1, 1' -dioctadecyl- 3,3,3'.3' tetramethylindocarbocyanine (DiI; Molecular Probes, Eugene, OR, USA). Fluorescent lipophilic tracer was added at 5 μL/mL in DMEM. After incubation for 20 min at 37°C with 5% humidified CO_2, the cells were centrifuged at 1,200 rpm for 5 min and washed twice with PBS. Fluorescence microscopy was used to investigate the survival and localization of transplanted cells.

10. Statistical analysis

In vitro Ca^{2+} concentration assay was analyzed by unpaired *t*-test. *In vivo* analyses were performed by unpaired *t*-test. A value of $P < 0.05$ was considered statistically significant.

Results

1. *In vitro* characterization of rat adipose-derived stromal cells

The cells from F344 (n = 4) and SD (n = 3) rats were capable of expanding *in vitro* and formed a heterogeneous population that morphologically resembled fibroblast-like cells (Fig. 3A).

The differentiation potential of each cell population was analyzed by culturing the cells under specific culture conditions that were favorable for adipogenic, chondrogenic or osteogenic differentiation. The accumulation of lipid vacuoles as determined by positive Oil red O staining was observed within the cytoplasm in all samples when subjected to adipogenic differentiation (Fig. 3A). The osteogenic differentiation potential was determined by ALP and Alizarin Red S staining (Fig. 3B). ALP activity increased at day 3 after culture in both cell populations with or without differentiation-inducing medium. In addition, osteogenic differentiation was demonstrated by the formation of Alizarin Red-positive mineralized nodules and measurement of calcium concentration in the extracellular matrix ($P < 0.05$) (Fig. 3C). All samples showed a similar potential for osteogenic differentiation. These results indicate that cells obtained from both the F344 rats and SD rats have the ability to differentiate into multiple mesenchymal cell lineages. Futhermore the newly synthesized glycosaminoglycan or proteoglycan as determined by positive Alcian Blue staining was observed in all samples when subjected to chondrogenic differentiation (Fig. 4).

2. Micro-CT analysis

Four F344 and three SD rats were analyzed using micro-CT at 1, 2, and 5 weeks after the transplantation procedure, without sacrifice, to determine the level of mineralization (Fig. 5). No visible adverse reactions, including root exposure, infection, or suppuration, were observed during the time prior to sacrifice of the rats, which was five weeks after surgery. In addition, neither ankylosis nor root resorption was observed in any of the samples. Consistently greater formation of supporting mineralized tissue around the tooth root was observed in all ASCs/PLGA groups than in PLGA-alone groups.

After one week, minor bone formation was observed at the wound margins in the ASCs/PLGA groups obtained from F344 and SD rats. After two weeks, minor bone formation was finally visible at the defect edges in PLGA groups from both F344 and SD rats. Interestingly, the ASCs/PLGA groups showed similar amounts of new bone formation and the newly formed bone was visible in the center of the defect as well as at the defect edges and covering the surface of the tooth root. The bone ingrowth from the residual bone was observed after five weeks in the PLGA groups. Micro-CT results showed that full bone formation was achieved in the ASCs/PLGA group defects in F344 and SD rats. A transmitted image was observed between the denuded root surface and alveolar bone in all groups, as demonstrated by frontal plane sectioning (Fig. 5). In addition, after five weeks there was a significant difference in the total amount of mineralized tissue

formation in the ASCs/PLGA groups from F344 and SD rats compared with the PLGA groups ($P < 0.05$) (Fig. 6).

3. Transplantation of ASCs/PLGA enhanced periodontal tissue regeneration

During creation of the periodontal defect, cementum was completely removed together with the supporting bone, which occasionally resulted in a penetration into the root dentin (Fig. 2D). At five weeks after surgery, the defect sites were easily identifiable in all groups by H-E. These demonstrated a smooth demarcation line representing the margin of the wound. At low magnification, formation of mineralized tissues and the remnants of the transplanted scaffolds were evident in all specimens at five weeks postsurgery (Fig. 7A, 7E, 7I and 7L). In addition, no apparent differences were observed in the newly formed periodontal tissue structures between F344 and SD rats. Indeed, these structures appeared similar in architecture to the original periodontal tissue, although the scaffold-alone groups showed less formation of the cementum-like layer, alveolar bone-like layer, and connective tissue layer compared with the ASCs/PLGA groups (Fig. 7B, 7F, 7J and 7M).

ASCs/PLGA groups demonstrated greater formation of bone-like structures within the defect, which coalesced with surrounding alveolar bone (Fig. 7G and 7M). The presence of osteoblasts lining the organic matrix and osteocytes trapped in the lacunae of newly formed bone structures were detected in the ASCs/PLGA group (Fig. 7G). In contrast, the defects in the PLGA groups were shown to have minimal formation of new bone-like structures and the newly formed bone was not in contact with the surrounding bone (Fig. 7C and 7J). Vascularization was seen in all samples.

Ligament tissue organization was recognized within the cementum-ligament- alveolar bone complex in all groups (Fig. 7B, 7F, 7J and 7M). The orientation of the ligament resembled the oblique functional orientation of the natural periodontal ligament structure. In the ASCs/PLGA groups, densely organized collagen fibers that were attached perpendicularly to the cementum layer were visualized by Picro Sirius Red staining (Fig. 7H and 7N). In the PLGA-alone groups, sparse and disorganized collagen fibers were observed (Fig. 7D and 7K).

The results of the histometric analysis from F344 rats are summarized in Fig. 8. The newly formed cementum in the ASCs/PLGA group was significantly thicker than that of the PLGA group in all areas of the periodontal tissue defects, including tooth crown, central, and the root apex ($P < 0.01$) (Fig. 8A). Furthermore, the periodontal ligament score in the ASCs/PLGA group was higher than that of the PLGA group in both tooth crown and central area of the periodontal tissue defects ($P < 0.05$) (Fig. 8B).

4. Localization of transplanted ASCs in the periodontal tissue defects

The newly formed acellular cementum layer, alveolar bone, and periodontal ligament were observed in periodontal wound site by H-E (Fig. 9A). DiI-labeled ASCs were easily visualized in the regenerated periodontal-like tissues in the wound site of the ASCs/PLGA groups (Fig. 9B).

Disucussion

The aim of the study was to evaluate the performance of PLGA-based solid scaffold seeded with rat ASCs, in enhancing periodontal tissue regeneration in surgically created periodontal defects (25). The development of a strategy for the regeneration of periodontal tissue is of major importance, as loss of this tissue results in tooth loss. Several strategies such as guided tissue/bone regeneration and the use of various growth factors have shown promise in promoting the tissue regeneration; however the establishment of a strategy for complete periodontal tissue regeneration is especially challenging. The major difficulty is in functional regeneration of the three tissues: cementum, periodontal ligament, and bone. Another difficulty lies in the fact that the healthy periodontal ligament harbors a niche for MSCs that plays key roles in the maintenance of regenerative capacity. In a diseased periodontal environment, the damaged tissue does not naturally repair because of the lack of MSCs. Transplanted MSCs might thus participate in the repair of damaged tissue and regulate regeneration via secretion of trophic factors or they could directly participate in regeneration of the periodontium (6, 36). For the functional repair of the cementum-ligament-bone complex, fibrous connective tissues are required to insert into the cementum and bone tissues to obtain an optimal biomechanical integration. In this study, I specifically observed the fibrous connective tissues by using Picro Sirius Red staining as well as H-E staining.

A successful tissue-engineering strategy requires the selection of a suitable cell source and a scaffold to maintain the space for cell growth and differentiation. MSCs from bone marrow, periodontal ligament, dental follicle, and adipose tissue have been described for potential use in periodontal regeneration (3, 15, 17, 30, 39, 62). Of these, ASCs are more similar to periodontal ligament-derived MSCs and demonstrate a better proangiogenic effect than MSCs from bone marrow (23, 24, 28). The effect is mediated by secretion of trophic factors from the transplanted ASCs as well as trans-differentiation into endothelial cells (37). Previous reports suggest that ASCs may be a suitable cell source for periodontal tissue regeneration because neovascularization is crucial for repair of periodontal tissue.

In this study, ASCs demonstrated osteogenic differentiation potential *in vitro* that is consistent with previous studies (18, 32, 58). Furthermore, the ASCs recently demonstrated the potential to differentiate into cementoblast-lineage cells in a cementogenic microenvironment *in vitro* (59). Cementoblasts show many phenotypic similarities to osteoblasts (1, 2, 9), and the present results suggested that ASCs may be capable of differentiating along the cementoblast lineage under specific microenvironmental conditions.

A scaffold suitable for periodontal tissue regeneration should be biodegradable such that it could be eventually replaced by regenerated tissue (50). In addition, the scaffold must be able to maintain a space within the wound site for the cells to grow into (5). Although use of soft scaffolds such as hydro gels or

collagen sponge has been the predominant strategy (8, 20, 29, 42, 54, 64), use of these soft scaffolds are limited due to their poor mechanical properties. Solid scaffolds such as hydroxyapatite/Tricalcium phosphate (HA/TCP) provide improved support for periodontal tissue regeneration (7, 33). However, the degradation period of HA/TCP may be too prolonged and the remnants of HA/TCP may influence the remodeling of the periodontium.

The *in vivo* performance of a complex of PLGA-based solid scaffold (PLGA-scaffod) and ASCs was examined. PLGA-scaffolds used in this study had fully interconnected pores and the larger pore size promoted the most cell ingrowth (19). In terms of mechanical properties, the PLGA-scaffolds had significantly higher compressive strength than other PLGA-based sponge-like scaffolds (data not shown). In this study, the PLGA-scaffolds were able to maintain their structural integrity for five weeks when used for *in vivo* transplants. In addition, the attachment of fibrous connective tissues to regenerated cementum and bone was observed in the defect. These results suggested that the PLGA-scaffolds used in this study have several advantages in periodontal tissue regeneration.

In addition, micro-CT results demonstrated that regeneration of tooth-supporting periodontal tissues in a periodontal tissue defect was enhanced when ASCs were seeded onto the PLGA-scaffold compared to PLGA-scaffold alone. In this study, micro-CT experiments were performed over time for all samples. Interestingly, in the PLGA-scaffold-only experiments, the healing pattern in terms of bone formation started only from the margins of the defect, and this was significantly different from the ASCs/PLGA groups, wherein bone formation was observed in the center of the defect as well as the margins. Based on this finding, early bone formation appears to occur more reliably in the ASCs/PLGA groups.

Periodontal tissue regeneration including cementum, periodontal ligament, and alveolar bone was observed in both inbred and outbred rats via *in vivo* studies. In all samples, neither rejection nor tissue damage were observed in the allogeneic transplantation model. In addition, no marked difference was observed between the periodontal regenerative capacity of autologous and allogeneic ASCs. This is consistent with previous findings using MSCs derived from periodontal ligament (14) and from bone marrow (21, 60). The present result support the concept that allogeneic ASCs may be a viable cell source.

A potential issue may be raised with regard to the promotion of periodontal tissue regeneration, as the fate of ASCs remains unclear. To address this issue, ASCs were treated with DiI before implantation, for cell tracking purposes. The labeling of transplanted cells facilitates assessment of cell migration into the healing periodontal wounds. This study was not successful to determine specifically whether the labeled ASCs generated the differentiated cementoblasts, osteoblasts, and periodontal ligament fibroblasts; however, labeled cells were observed mainly in the fibrobrast connective tissue. Further study is needed to identify whether ASCs have the potential to differentiate into hard tissue-forming cell.

Conclusions

The aim of this study was to assess the efficacy of a combination of ASCs and PLGA-scaffolds in repairing periodontal tissue defects. The following conclusions were obtained.

1. Cultured ASCs showed adipogenic, osteogenic and chondrogenic differentiation.

2. Transplantaion of PLGA-scaffolds with ASCs enhanced hard tissue formation in the periodontal tissue defects.

3. The regenerated periodontal tissue showed the original architecture, with collagen fibers inserted into the cementum and bone layers.

4. DiI-labeled ASCs were located in the regenerated periodontal-like tissues in the wound site.

These results indicate that transplanted ASCs promoted periodontal tissue regeneration, and that the PLGA-scaffolds may prevent gingival invasion by securing a space for periodontal tissue regeneration. Collectively, transplantation of ASCs in combination with PLGA-scaffold has sufficient potential for periodontal tissue reconstruction.

Acknowledgements

This work was supported in part by Grant-in-Aid for Scientific Research (B) (21390528 & 24390447 to Honda M), Grant from Dental Research Center (Honda M), Nihon University School of Dentistry, and Nihon University Multidisciplinary Research Grant for 2012 and 2013 (Honda M).

References

1) Arrigoni E, Lopa S, de Girolamo L, Stanco D and Brini AT (2009) Isolation, characterization and osteogenic differentiation of adipose-derived stem cells: from small to large animal models. Cell Tissue Res 338, 401-411.
2) Bosshardt D.D (2005) Are cementoblasts a subpopulation of osteoblasts or a unique phenotype? J Dent Res 84, 390-406.
3) Caton J, Bostanci N, Remboutsika E, De Bari C and Mitsiadis TA (2011) Future dentistry: cell therapy meets tooth and periodontal repair and regeneration. J Cell Mol Med 15, 1054-1065.
4) Chen FM and Jin Y (2010) Periodontal tissue engineering and regeneration: current approaches and expanding opportunities. Tissue Eng Part B Rev 16, 219-255.
5) Chen FM, Zhang J, Zhang M, An Y, Chen F and Wu ZF (2010) A review on endogenous regenerative technology in periodontal regenerative medicine. Biomaterials 31, 7892-7927.
6) Chen SC, Marino V, Gronthos S and Bartold PM (2006) Location of putative stem cells in human periodontal ligament. J Periodontal Res 41, 547-553.
7) Ding G, Liu Y, Wang W, Wei F, Liu D, Fan Z, An Y, Zhang C and Wang S (2010) Allogeneic periodontal ligament stem cell therapy for periodontitis in swine. Stem Cells 28, 1829-1838.
8) Doğan A, Ozdemir A, Kubar A and Oygür T (2003) Healing of artificial fenestration defects by seeding of fibroblast-like cells derived from regenerated periodontal ligament in a dog: a preliminary study. Tissue Eng 9, 1189-1196.
9) Elabd C, Chiellini C, Massoudi A, Cochet O, Zaragosi LE, Trojani C, Michiels JF, Weiss P, Carle G, Rochet N, Dechesne CA, Ailhaud G, Dani C and Amri EZ (2007) Human adipose tissue-derived multipotent stem cells differentiate *in vitro* and *in vivo* into osteocyte-like cells. Biochem Biophys Res Commun 361, 342-348.
10) Gimble J and Guilak F (2003) Adipose-derived adult stem cells: isolation, characterization, and differentiation potential. Cytotherapy 5, 362-369.
11) Gimble JM, Katz AJ and Bunnell BA (2007) Adipose-derived stem cells for regenerative medicine. Circ Res 100, 1249-1260.
12) Hammarstrom L (1997) Enamel matrix, cementum development and regeneration. J Clin Periodontol 24, 658-668.
13) Hammarstrom L, Heijl L and Gestrelius S (1997) Periodontal regeneration in a buccal dehiscence model in monkeys after application of enamel matrix proteins. J Clin Periodontol 24, 669-677.
14) Han J, Menicanin D, Marino V, Ge S, Mrozik K, Gronthos S and Bartold PM (2013) Assessment of the regenerative potential of allogeneic periodontal ligament stem cells in a rodent periodontal defect model. J Periodontal Res, doi: 10.1111/jre.12111.
15) Honda MJ, Imaizumi M, Tsuchiya S and Morsczeck C (2010) Dental follicle stem cells and tissue engineering. J Oral Sci 52, 541-552.
16) Huang JI, Zuk PA, Jones NF, Zhu M, Lorenz HP, Hedrick MH and Benhaim P (2004) Chondrogenic potential of multipotential cells from human adipose tissue. Plast Reconstr Surg 113, 585-594.
17) Hynes K, Menicanin D, Gronthos S and Bartold PM (2012) Clinical utility of stem cells for periodontal regeneration. Periodontol 2000 59, 203-227.
18) Inanc B, Elcin AE and Elcin YM (2006) Osteogenic induction of human periodontal

ligament fibroblasts under two- and three-dimensional culture conditions. Tissue Eng 12, 257-266.
19) Itoh S, Nakamura S, Nakamura M, Shinomiya K and Yamashita K (2006) Enhanced bone ingrowth into hydroxyapatite with interconnected pores by electrical polarization. Biomaterials 27, 5572-5579.
20) Kawaguchi H, Hirachi A, Hasegawa N, Iwata T, Hamaguchi H, Shiba H, Takata T, Kato Y and Kurihara H (2004) Enhancement of periodontal tissue regeneration by transplantation of bone marrow mesenchymal stem cells. J Periodontol 75, 1281-1287.
21) Keilhoff G, Goihl A, Stang F, Wolf G and Fansa H (2006) Peripheral nerve tissue engineering: autologous Schwann cells vs. transdifferentiated mesenchymal stem cells. Tissue Eng 12, 1451-1465.
22) Kilroy GE, Foster SJ, Wu X, Ruiz J, Sherwood S, Heifetz A, Ludlow JW, Stricker DM, Potiny S, Green P, Halvorsen YD, Cheatham B, Storms RW and Gimble JM (2007) Cytokine profile of human adipose-derived stem cells: expression of angiogenic, hematopoietic, and pro-inflammatory factors. J Cell Physiol 212, 702-709.
23) Kim SJ, Cho HH, Kim YJ, Seo SY, Kim HN, Lee JB, Kim JH, Chung JS and Jung JS (2005) Human adipose stromal cells expanded in human serum promote engraftment of human peripheral blood hematopoietic stem cells in NOD/SCID mice. Biochem Biophys Res Commun 329, 25-31.
24) Kim Y, Kim H, Cho H, Bae H, Suh K and Jung J (2007) Direct comparison of human mesenchymal stem cells derived from adipose tissues and bone marrow in mediating neovascularization in response to vascular ischemia. Cell Physiol Biochem 20, 867-876.
25) King GN, King N, Cruchley AT, Wozney JM and Hughes FJ (1997) Recombinant human bone morphogenetic protein-2 promotes wound healing in rat periodontal fenestration defects. J Dent Res 76, 1460-1470.
26) Kubo K, Tsukasa N, Iki K, Uehara M, Shimotsu A, Seto Y, Hyon SH, Ikada Y, Kubota T and Sueda T (1998) Occlusive effects of lactic acid-glycolic acid copolymer membrane on gingival fibroblasts in vitro. J Biomed Mater Res 39, 554-559.
27) Langer R and Vacanti JP (1993) Tissue engineering. Science 260, 920-926.
28) Lee RH, Kim B, Choi I, Kim H, Choi HS, Suh K, Bae YC and Jung JS (2004) Characterization and expression analysis of mesenchymal stem cells from human bone marrow and adipose tissue. Cell Physiol Biochemy 14, 311-324.
29) Li H, Yan F, Lei L, Li Y and Xiao Y (2009) Application of autologous cryopreserved bone marrow mesenchymal stem cells for periodontal regeneration in dogs. Cells Tissues Organs 190, 94-101.
30) Lin NH, Gronthos S and Bartold PM (2009) Stem cells and future periodontal regeneration. Periodontol 2000 51, 239-251.
31) Lindhe J, Pontoriero R, Berglundh T and Araujo M (1995) The effect of flap management and bioresorbable occlusive devices in GTR treatment of degree III furcation defects. An experimental study in dogs. J Clin Periodontol 22, 276-283.
32) Liu Q, Cen L, Zhou H, Yin S, Liu G, Liu W, Cao Y and Cui L (2009) The role of the extracellular signal-related kinase signaling pathway in osteogenic differentiation of human adipose-derived stem cells and in adipogenic transition initiated by dexamethasone. Tissue Eng Part A 15, 3487-3497.
33) Liu Y, Zheng Y, Ding G, Fang D, Zhang C, Bartold PM, Gronthos S, Shi S and. Wang S (2008) Periodontal ligament stem cell-mediated treatment for periodontitis in miniature swine. Stem Cells 26, 1065-1073.
34) Lu F, Mizuno H, Uysal CA, Cai X, Ogawa R and Hyakusoku H (2008) Improved

viability of random pattern skin flaps through the use of adipose-derived stem cells. Plast Reconstr Surg 121, 50-58.
35) Matsumoto T, Kano K, Kondo D, Fukuda N, Iribe Y, Tanaka N, Matsubara Y, Sakuma T, Satomi A, Otaki M, Ryu J and Mugishima H (2008) Mature adipocyte-derived dedifferentiated fat cells exhibit multilineage potential. J Cell Physiol 215, 210-222.
36) Mikami Y, Ishii Y, Watanabe N, Shirakawa T, Suzuki S, Irie S, Isokawa K and Honda MJ (2011) CD271/p75(NTR) inhibits the differentiation of mesenchymal stem cells into osteogenic, adipogenic, chondrogenic, and myogenic lineages. Stem Cells Dev 20, 901-913.
37) Moon MH, Kim SY, Kim YJ, Kim SJ, Lee JB, Bae YC, Sung SM and Jung JS (2006) Human adipose tissue-derived mesenchymal stem cells improve postnatal neovascularization in a mouse model of hindlimb ischemia. Cell Physiol Biochem 17, 279-290.
38) Mooney DJ and Vandenburgh H (2008) Cell delivery mechanisms for tissue repair. Cell Stem Cell 2, 205-213.
39) Morsczeck C, Schmalz G, Reichert TE, Völlner F, Galler K and Driemel O (2008) Somatic stem cells for regenerative dentistry. Clin Oral Investig 12, 113-118.
40) Nakagami H, Morishita R, Maeda K, Kikuchi Y, Ogihara T and Kaneda Y (2006) Adipose tissue-derived stromal cells as a novel option for regenerative cell therapy. J Atheroscler Thromb 13, 77-81.
41) Nakahara T (2006) A review of new developments in tissue engineering therapy for periodontitis. Dent Clin North Am 50, 265-276.
42) Nuñez J, Sanz-Blasco S, Vignoletti F, Muñoz F, Arzate H, Villalobos C, Nuñez L, Caffesse RG and Sanz M (2012) Periodontal regeneration following implantation of cementum and periodontal ligament-derived cells. J Periodontal Res 47, 33-44.
43) Nyman S, Lindhe J, Karring T and Rylander H (1982) New attachment following surgical treatment of human periodontal disease. J Clin Periodontol 9, 290-296.
44) Park JB, Matsuura M, Han KY, Norderyd O, Lin WL, Genco RJ and Cho MI (1995) Periodontal regeneration in class III furcation defects of beagle dogs using guided tissue regenerative therapy with platelet-derived growth factor. J Periodontol 66, 462-477.
45) Pittenger MF, Mackay AM, Beck SC, Jaiswal RK, Douglas R, Mosca JD, Moorman MA, Simonetti DW, Craig S and Marshak DR (1999) Multilineage potential of adult human mesenchymal stem cells. Science 284, 143-147.
46) Planat-Benard V, Silvestre JS, Cousin B, André M, Nibbelink M, Tamarat R, Clergue M, Manneville C, Saillan-Barreau C, Duriez M, Tedgui A, Levy B, Pénicaud L and Casteilla L (2004) Plasticity of human adipose lineage cells toward endothelial cells: physiological and therapeutic perspectives. Circulation 109, 656-663.
47) Prockop DJ (1997) Marrow stromal cells as stem cells for nonhematopoietic tissues. Science 276, 71-74.
48) Rehman J, Traktuev D, Li J, Merfeld-Clauss S, Temm-Grove CJ, Bovenkerk JE, Pell CL, Johnstone BH, Considine RV and March KL (2004) Secretion of angiogenic and antiapoptotic factors by human adipose stromal cells. Circulation 109, 1292-1298.
49) Reyes M, Dudek A, Jahagirdar B, Koodie L, Marker PH and Verfaillie CM (2002) Origin of endothelial progenitors in human postnatal bone marrow. J Clin Invest 109, 337-346.
50) Rungsiyanont S, Dhanesuan N, Swasdison S and Kasugai S (2012) Evaluation of biomimetic scaffold of gelatin-hydroxyapatite crosslink as a novel scaffold for tissue engineering: biocompatibility evaluation with human PDL fibroblasts, human

mesenchymal stromal cells, and primary bone cells. J Biomater Appl 27, 47-54.
51) Safford KM, Hicok KC, Safford SD, Halvorsen YD, Wilkison WO, Gimble JM and Rice HE (2002) Neurogenic differentiation of murine and human adipose-derived stromal cells. Biochem Biophys Res Commun 294, 371-379.
52) Strem BM, Hicok KC, Zhu M, Wulur I, Alfonso Z, Schreiber RE, Fraser JK and Hedrick MH (2005) Multipotential differentiation of adipose tissue-derived stem cells. Keio J Med 54, 132-141.
53) Tobita M, Orbay H and Mizuno H (2011) Adipose-derived stem cells: current findings and future perspectives. Discov Med 11, 160-170.
54) Tobita M, Uysal AC, Ogawa R, Hyakusoku H amd Mizuno H (2008) Periodontal tissue regeneration with adipose-derived stem cells. Tissue Eng Part A 14, 945-953.
55) Tobita M, Uysal CA, Guo X, Hyakusoku H and Mizuno H (2013) Periodontal tissue regeneration by combined implantation of adipose tissue-derived stem cells and platelet-rich plasma in a canine model. Cytotherapy 15, 1517-26.
56) Trombelli L (2005) Which reconstructive procedures are effective for treating the periodontal intraosseous defect? Periodontol 2000 37, 88-105.
57) Wang HL, Greenwell H, Fiorellini J, Giannobile W, Offenbacher S, Salkin L, Townsend C, Sheridan P, Genco RJ; Research, Science and Therapy Committee (2005) Periodontal regeneration. J Periodontol 76, 1601-1622.
58) Wang Q, Steigelman MB, Walker JA, Chen S, Hornsby PJ, Bohnenblust ME and Wang HT (2009) In vitro osteogenic differentiation of adipose stem cells after lentiviral transduction with green fluorescent protein. J Craniofac Surg 20, 2193-2199.
59) Wen X, Nie X, Zhang L, Liu L and Deng M (2011) Adipose tissue-deprived stem cells acquire cementoblast features treated with dental follicle cell conditioned medium containing dentin non-collagenous proteins *in vitro*. Biochem Biophys Res Commun 409, 583-589.
60) Xiang Z, Liao R, Kelly MS and Spector M (2006) Collagen-GAG scaffolds grafted onto myocardial infarcts in a rat model: a delivery vehicle for mesenchymal stem cells. Tissue Eng 12, 2467-2478.
61) Yang Y, Rossi FM and Putnins EE (2010) Periodontal regeneration using engineered bone marrow mesenchymal stromal cells. Biomaterials 31, 8574-8582.
62) Yoshida T, Washio K, Iwata T, Okano T and Ishikawa I (2012) Current status and future development of cell transplantation therapy for periodontal tissue regeneration. Int J Dent 2012, 307024.
63) Zaragosi LE, Ailhaud G and Dani C (2006) Autocrine fibroblast growth factor 2 signaling is critical for self-renewal of human multipotent adipose-derived stem cells. Stem Cells 24, 2412-2419.
64) Zhao M, Jin Q, Berry JE, Nociti FH Jr, Giannobile WV and Somerman MJ (2004) Cementoblast delivery for periodontal tissue engineering. J Periodontol 75, 154-161.
65) Zuk PA, Zhu M, Ashjian P, De Ugarte DA, Huang JI, Mizuno H, Alfonso ZC, Fraser JK, Benhaim P and Hedrick MH (2002) Human adipose tissue is a source of multipotent stem cells. Mol Biol Cell 13, 4279-4295.
66) Zuk PA, Zhu M, Mizuno H, Huang J, Futrell JW, Katz AJ, Benhaim P, Lorenz HP and Hedrick MH. (2001) Multilineage cells from human adipose tissue: implications for cell-based therapies. Tissue Eng 7, 211-228.

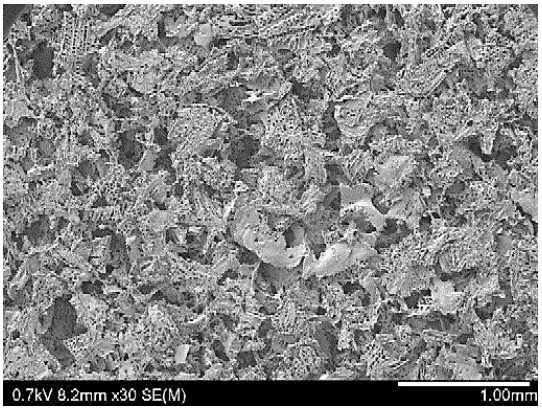

Fig. 1 SEM images of the PLGA-based solid scaffold (PLGA-scaffold).

The mean size of the interconnected pore was approximately 200 μm.

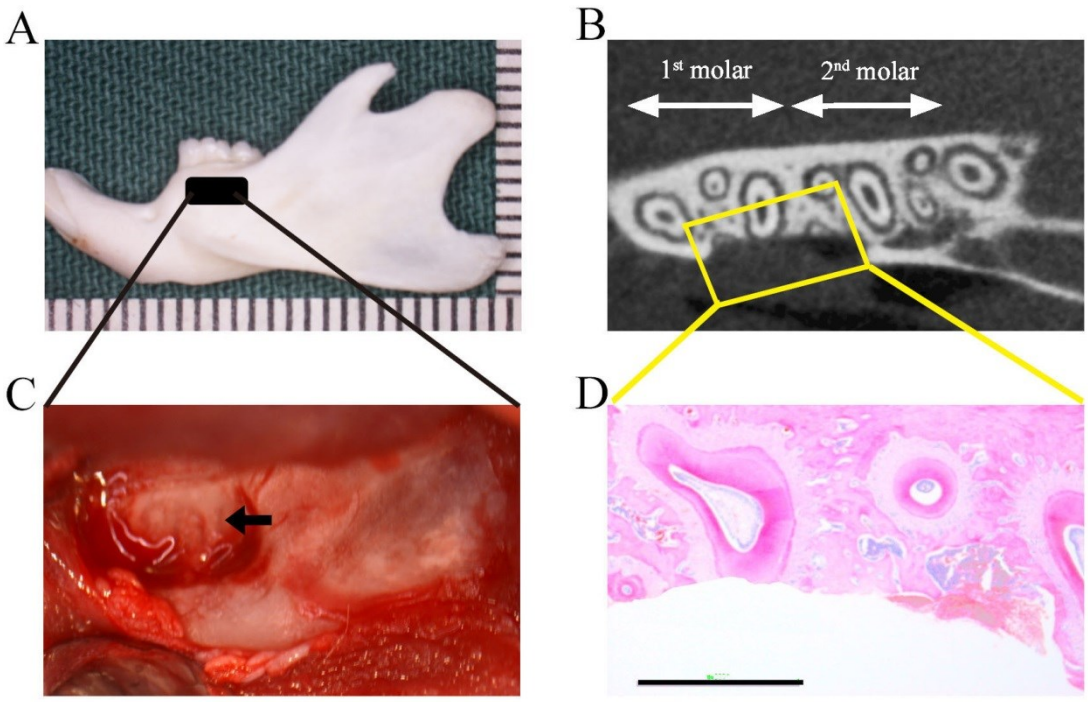

Fig. 2 Preparation of the rat periodontal defect model.
(A) Example of a rat mandibular bone used to create the periodontal defects. The black box indicates the surgically created periodontal defect on the buccal surface of the mandible.
(B) Micro-CT image of a rat periodontal-tissue defect immediately after surgery.
(C) Macroscopic view of a surgically created periodontal-tissue defect on the buccal surface of the mandibular first and second molars. The defect includes the cementum, alveolar bone, and periodontal ligament, and the distal root of the mandibular first molar is exposed (black arrow).
(D) H-E staining of the surgically exposed distal root of the first molar in the rat mandible showed loss of cementum, alveolar bone, and periodontal ligament (Scale bar: 1000 μm).

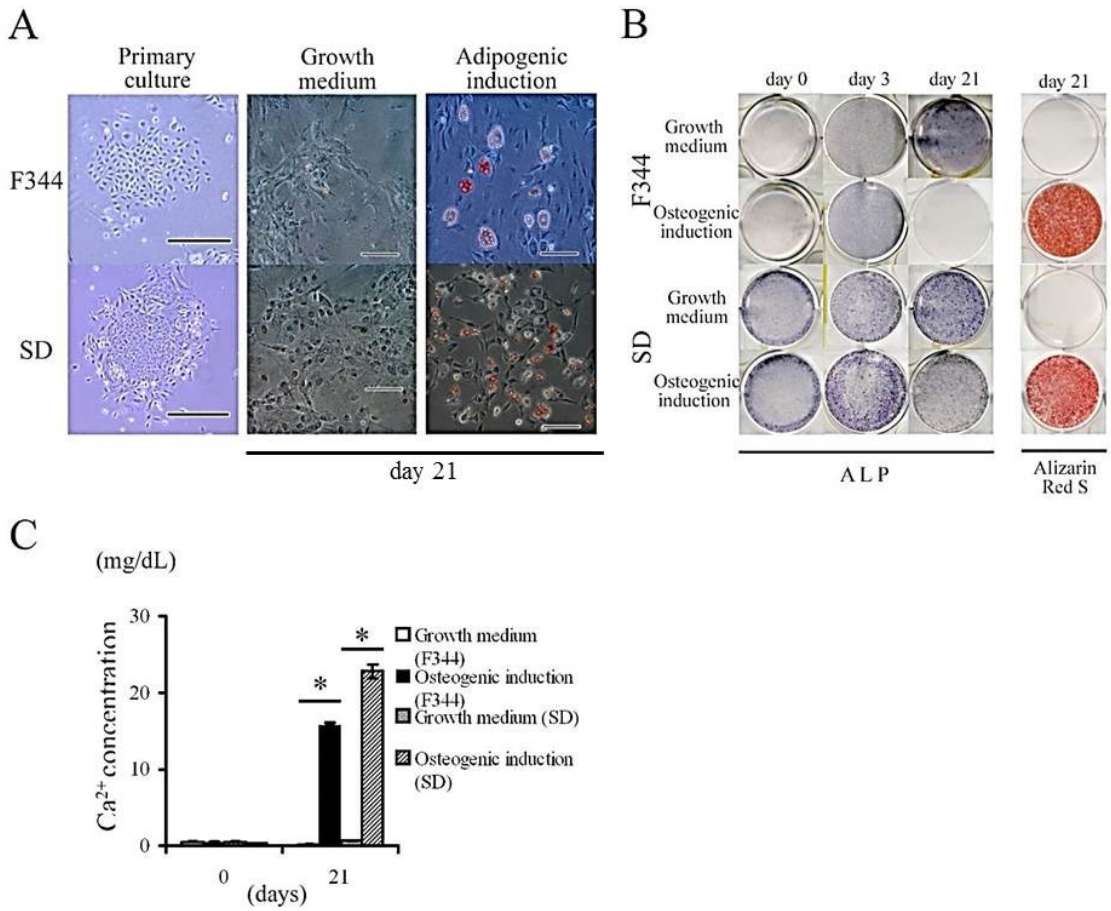

Fig. 3 *In vitro* characterization of adipose-derived stromal cells (ASCs).

(A) Microscopic view of primary cultured ASCs harvested from rat inguinal fat pads in inbred F344 rats or outbred SD rats. Both ASCs cultures showed clonogenic potential for 7 days culture in growth medium (Scale bar: 500 μm). ASCs were further cultured 3 weeks in either growth medium or adipogenic induction medium. Oil red O staining identified lipid vacuoles in the ASCs in adipogenic differentiation medium (Scale bars: 100 μm).

(B) After confluence, ASCs from F344 and SD rats were cultured for 3 weeks in either growth medium or osteogenic induction medium. Cells were stained with ALP and with Alizarin red S. Mineralized nodules were observed in the cells after 21 days of culture in osteogenic induction medium.

(C) Calcium concentration was determined by quantitative colorimetric assay. Each bar represents the mean ± SD (n = 4 in each group); $*P < 0.05$, compared to the cells in growth medium (unpaired *t* test).

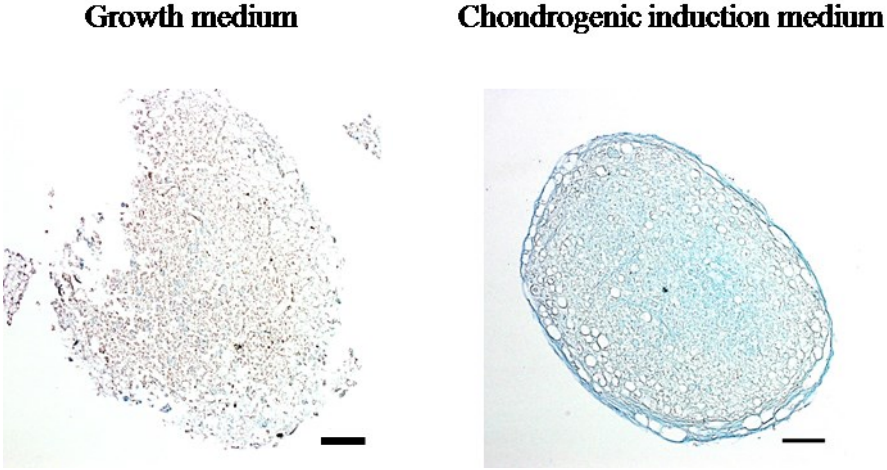

Fig. 4　Chondrogenic differentiation of ASCs.
After ASCs obtained from F344 rats were cultured for 21 days in either growth medium or chondrogenic induction medium, ASCs were stained with Alcian Blue to evaluate chondrogenic differentiation potential (Scale bar: 100 μm).

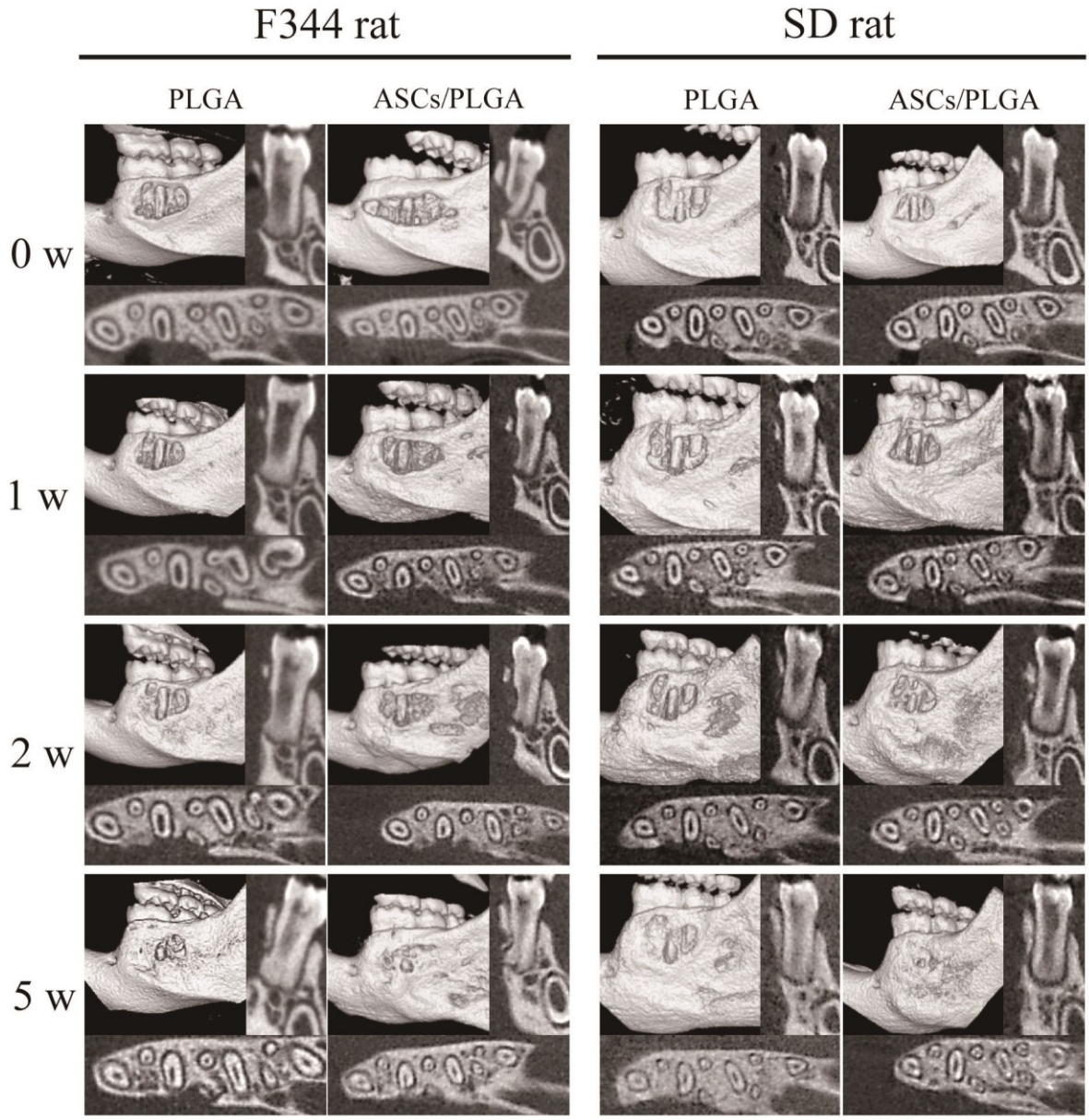

Fig. 5　Continuous micro-CT analysis at 1, 2, and 5 weeks after cell transplantation. Micro-CT images were obtained from same F344 (n = 4) or SD (n = 3) rats immediately after surgery, and at 1, 2, and 5 weeks after surgery. 3D images were reconstructed using i-View. No ankylosis or root resorption was observed in any of the samples. Regeneration of mineralized tissue in the periodontal-tissue defects was observed at 2 weeks after surgery. The ASCs/PLGA combination promoted more mineralized tissue regeneration than the PLGA alone. At 5 weeks after surgery, newly formed bone covered most of the buccal dental root in the ASCs/PLGA groups.

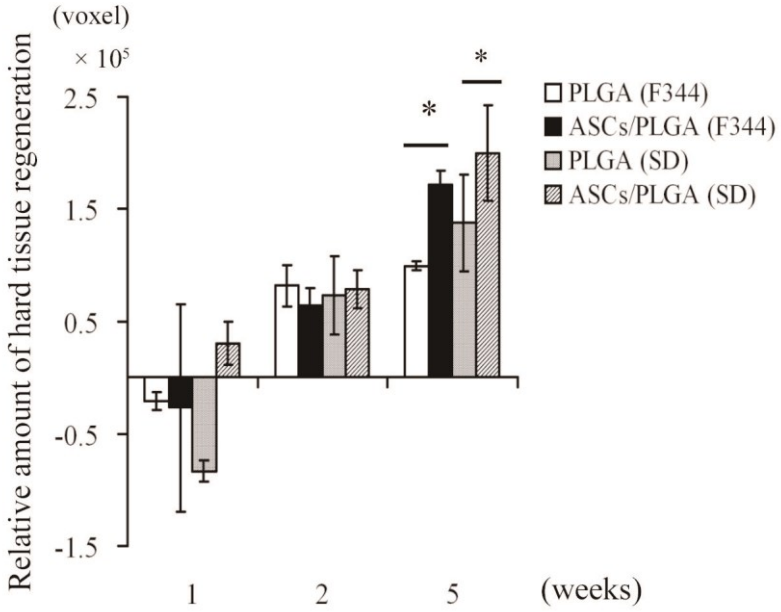

Fig. 6　Newly formed mineralized tissue volume by micro-CT analysis.
The volume of newly formed mineralized tissue was calculated using 3by4viewer2011. At 5 weeks after surgery, a significant difference was observed between ASCs/PLGA and PLGA-alone groups in both F344 (n = 4, $*P < 0.05$) and SD rat experiments (n = 3, $*P < 0.05$).

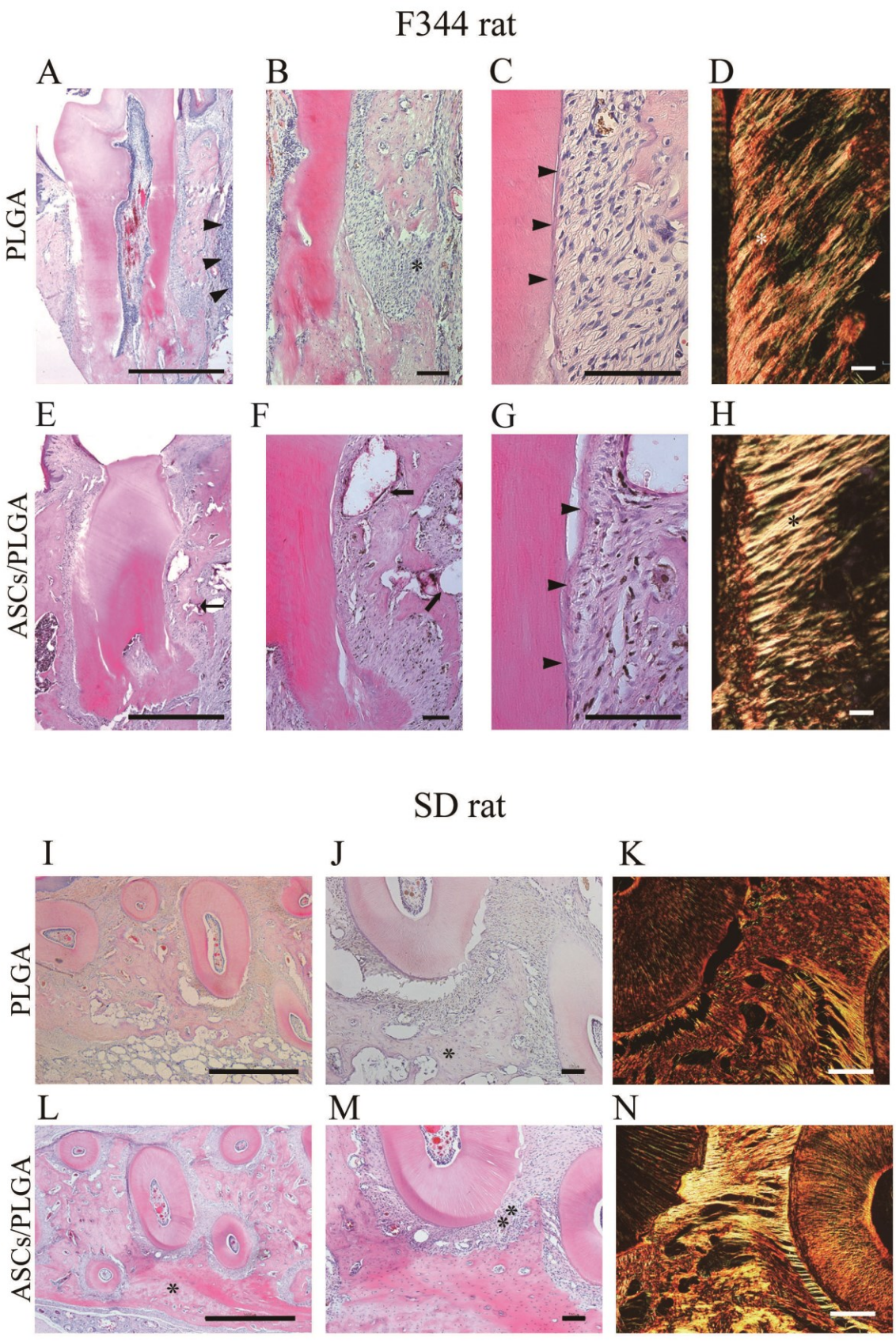
F344 rat
A
B
C
D
PLGA
E
F
G
H
ASCs/PLGA
SD rat
I
J
K
PLGA
L
M
N
ASCs/PLGA

Fig. 7　Hematoxylin and eosin-stained frontal plane (A-H) and horizontal (I-N) sections of the periodontal-tissue defects at 5 weeks after surgery.
(A, E) Frontal plane sections show newly bone formation in the periodontal tissue defects. Extensive inflammatory cell infiltration can be seen at the outer edge of the newly formed bone in the PLGA-alone group (black arrowheads). ASCs/PLGA group shows continuous, new alveolar bone in the periodontal-tissue defect (black arrow) and maintenance of the space between the dental root and newly formed alveolar bone (Scale bar: 1000 μm).
(B, F) No bone formation was also observed at this time point in the periodontal-tissue defect in the PLGA-alone group (asterisk). The regenerated bone has clearly connected with the native alveolar bone in the ASCs/PLGA group. Black arrows indicate remnant of the transplanted scaffold in the periodontal-tissue defects (Scale bar: 100 μm).
(C, G) Higher magnification of the defect shows regenerated connective tissue layer oriented perpendicular to the newly formed cementum-like layer. The cementum layer was thicker in the ASCs/PLGA group than that in the PLGA-alone group (black arrowheads) (Scale bar: 100 μm).
(D, H) Picro Sirius red staining at higher magnification polarizing microscopy showed a non-dense collagen bundle (white asterisk) in the PLGA-alone group. Dense collagen bundles (black asterisk) can be seen attaching perpendicularly to the newly formed cementum in the ASCs/PLGA group (Scale bar: 10 μm).
(I, L) Horizontal sections show a periodontal-tissue space between the newly formed bone and root dentin in the PLGA-alone and ASCs/PLGA group. The width of regenerated bone (asterisk) in the periodontal-tissue defect was similar to that of native alveolar bone (Scale bar: 1000 μm).
(J, M) The newly formed bone (asterisk in J) is thinner in the PLGA-alone group than in the ASCs/PLGA group. The width of the space (double asterisk in M) occupied by regenerated periodontal ligament is maintained relative to that in the native periodontal ligament space in the ASCs/PLGA group (Scale bar: 100 μm).
(K, N) The regenerated collagen bundles are obliquely oriented to the dental-root surface, shown by Picro Sirius Red staining. A thick collagen bundle can be seen between the new cementum-like layer and the native cementum in an adjacent tooth in the ASCs/PLGA group, compared with a thinner bundle in the PLGA-alone group (Scale bar: 100 μm).

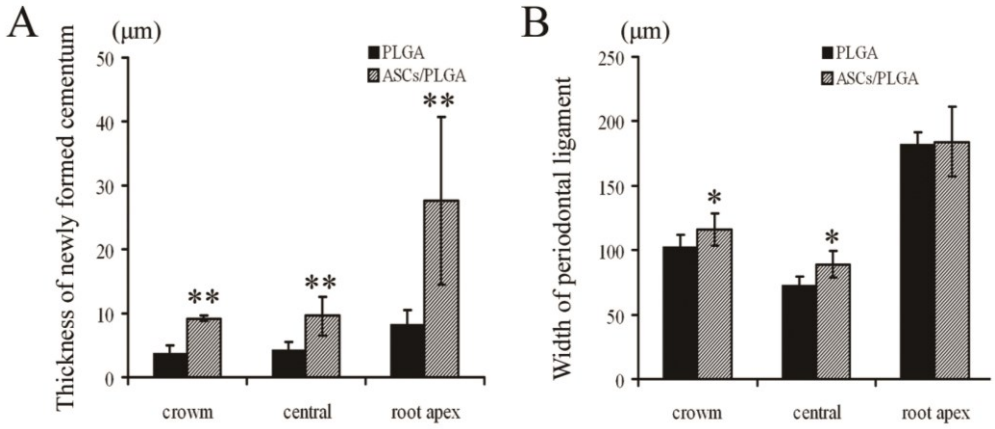

Fig. 8 Histometric analysis of the regenerated cementum and periodontal ligament.
(A) Histometric analyses of the thickness of new cementum and the regenerated periodontal ligament tissue width. Significantly more cementum was formed in the ASCs/PLGA group in all areas compared to the PLGA-alone group. Each bar represents the mean ± SD (n = 4); $^{**}P < 0.01$, compared to the PLGA group (unpaired *t* test).
(B) The width of newly formed periodontal ligament in the ASCs/PLGA group was significantly greater than in the PLGA-alone group in the tooth crown and central areas, whereas no difference was found in the root apex. Each bar represents the mean ± SD (n = 4); $^{*}P < 0.05$, compared to the PLGA-alone group (unpaired *t* test).

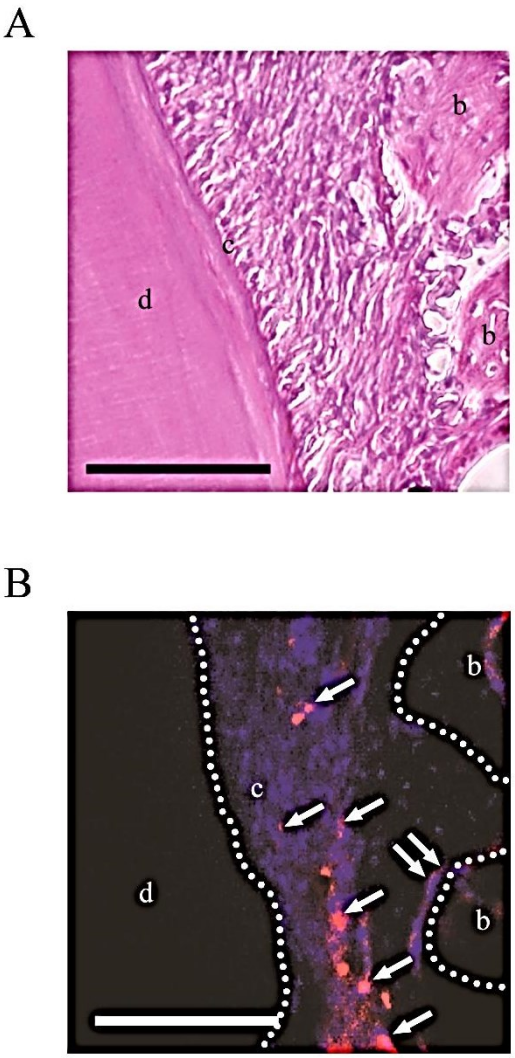

Fig. 9　Localization of transplanted ASCs using DiI analysis.
(A)　　A histological overview showed the periodontal tissue regeneration 2 week after ransplantation (H-E staining; scale bar: 100 μm).
(B)　　DiI labeled ASCs (white arrows) could be seen in the periodontal-tissue defects at 2 weeks after transplantation.　b: newly formed bone, c: newly formed cementum, d: root dentin, blue color: DAPI (Scale bar: 100 μm).